Wavelength and temperature performance of polarization-transforming fiber

Allen H. Rose, Nicolas Feat, and Shelley M. Etzel

We have theoretically and experimentally investigated an optical fiber with circular polarization modes on one end and linear polarization modes on the other end. We call this fiber a polarization-transforming fiber because the local modes, or polarization states they represent, are converted from linear to circular, and visa versa, in the fiber. We have developed and implemented a postdraw process for making polarization-transforming fiber samples 30 mm long with losses less than 1 dB and a polarization-mode conversion from circular to linear greater than 20 dB. Also, we have modeled and measured the dependence on wavelength and temperature of polarization-transforming fiber samples. The measured normalized wavelength dependence of a sample fiber 30 mm long was approximately 1.4×10^{-4} nm^{-1}, and the measured normalized temperature dependence was approximately 6×10^{-4} °C^{-1}. These values are better in some cases than values for conventional high-birefringent fiber quarter-wave plates.

OCIS codes: 060.0060, 060.2310, 230.0040, 230.5440.

1. Introduction

Conventional high-birefringent (hi-bi) fiber has only linear optical eigenmodes, and when a linear polarization state is launched into the hi-bi fiber on one of the axes of birefringence the linear polarization state is preserved, thus the name polarization-maintaining (PM) fiber. If hi-bi fiber is spun at a high enough rate, or at a short twist pitch, the fiber will have circular eigenmodes, preserving a circular polarization state launched into the fiber.[1] However, if a hi-bi fiber has a variable twist pitch along the length, the slow-spun (long twist pitch) end will have the properties of a PM fiber, linear local modes guiding linear polarization states, and the fast-spun (short twist pitch) end will have spun hi-bi properties, or circular local modes guiding circular polarization states. The variable-spun hi-bi fiber can couple linear polarization modes to circular polarization modes over its length. This has the effect of converting states of linear polarization into states of circular polarization, or visa versa. We choose to call this fiber a polarization-transforming (PT) fiber. A schematic of this concept is shown in Fig. 1.

PT fiber was first proposed by Huang,[2,3] who presented the mathematics used to solve the variably coupled-mode equations for this type of fiber and described the effects of such a modification on the fiber's optical properties. Huang showed that it was possible to predict the behavior of such a fiber, provided that certain physical conditions were fulfilled.[2,3] He proved the principle of this fiber by drawing variably spun hi-bi fiber and cutting the fiber at the fast- and slow-spun ends.[2] However, the majority of his experimental investigation was applicable only to lengths of fiber that were longer than 0.5 m. He briefly describes the shorter-length fibers, the postdraw manufacture method, and (to our knowledge) has not investigated the temperature and wavelength dependence of these fibers.[2,3]

In this paper we evaluate the wavelength and temperature performance of the PT fiber and compare it with a conventional birefringent fiber quarter-wave plate. To make a PT fiber component, we modified the physical properties of a hi-bi optical fiber, postdraw. We heat the fiber to a temperature near melting and then twist it, varying the twist rate from fast at one end down to zero at the other end. Because of the high temperatures used, elasto-optic effects do not come into play in this fiber. (See Section 2 for a discussion of the temperatures used.) Also we theoretically investigated the behavior of such a PT fiber

When this research was performed the authors were with the Division of Optoelectronics, National Institute of Standards and Technology, Boulder, Colorado 80305. A. H. Rose (arose@nxtphase.com) is now with NxtPhase, Incorporated, 2075 West Pinnicale Peak Road, Phoenix, Arizona 85027. N. Feat is now with Photon Kinetics Incorporated, Beaverton, Oregon 97008.

Received 9 October 2002; revised manuscript received 6 August 2003.

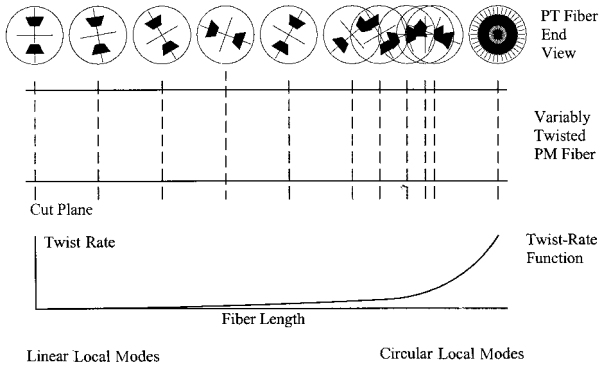

Fig. 1. Schematic diagram of a PT fiber showing the fiber's end view if cut at various points along the length. Also shown is the twist rate along the length of the fiber. At the slow-twist end the local modes are linear. At the fast-twist end the local modes are circular.

with the method of coupled-mode equations and for various twist-rate profiles and fiber lengths.[2]

The PT fiber can be compared with a conventional quarter-wave plate because it changes the polarization state of light passing through it, but there are subtle differences. To understand these differences, we first describe a conventional PM fiber quarter-wave plate. A PM fiber quarter-wave plate is made when a length of the PM fiber is prepared with a quarter of a beat length of birefringence. Launching the linearly polarized light into the fiber quarter-wave plate at 45° to the hi-bi axes will convert the linear polarization state into a circular state by the accumulated change in phase between the two linear eigenmodes. The device is bidirectional, meaning that linearly polarized light can be launched into either end; and as long as the orientation with the linear polarization state and the hi-bi axes is maintained, a circular polarization state results.

The PT fiber is not bidirectional in the same manner as the hi-bi fiber quarter-wave plate. If linearly polarized light is launched into the slow-spun end on the axis of the hi-bi fiber, then a circularly polarized beam of light will exit the fiber. If linearly polarized light is launched into the fast-spun end of the PT fiber at the appropriate angle (which is dependent on the fiber's twist rate and birefringence), the input state will be converted to a circularly polarized state at the slow-spun end. If linearly polarized light is launched into the fast-spun end at 45° to the hi-bi axes, the output will be some arbitrary polarization state dependent on the PT fiber length, twist rate, and birefringence. If circularly polarized light is launched into the slow-spun end, a linear state will exit; the angle of the linear state is dependent on the PT fiber parameters. If a right-circular polarization state is launched into the fast-spun end, the output at the slow-spun end of the fiber will be a linear polarization state on the horizontal axis. In all these cases the variable mode coupling strength and PM fiber axes determine the orientation of the output state. Another difference is the PT fiber uses many

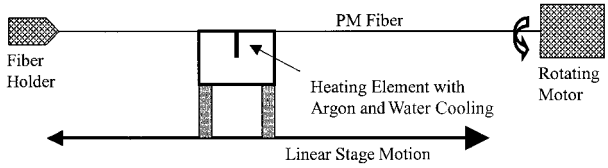

Fig. 2. Schematic diagram of the apparatus used to heat and twist the PM fiber into PT fiber samples. The PM fiber is held on the heating fixture by a vacuum V-groove. The tungsten heating element is cooled by an argon flow, and the heating fixture is cooled by water. The heating element, linear stage, and rotating motor are under computer control.

beat lengths of a PM fiber to accomplish the polarization-mode conversion, and the hi-bi fiber quarter-wave plate at a minimum will use only a quarter beat length. (For a more detailed description and theoretical evaluation of the different input–output arrangements of a PT fiber, see Huang.[2])

The PT fiber has some unique properties that can be used in some applications such as a conventional quarter-wave plate.[2] The temperature and wavelength dependencies of a PT fiber are affected by the spin-rate profile and length of the fiber and not directly on the change in the birefringence of the fiber with temperature and wavelength. Thus the temperature and wavelength dependencies of the PT fiber can be tailored. We show that in some cases the temperature and wavelength dependencies are many times smaller than those for the conventional PM fiber quarter-wave plate.

2. Apparatus for Polarization-Transforming Fiber Manufacture

To make short PT fiber samples, of the order of tens of millimeters in length, we heated and twisted a hi-bi fiber postdraw. A schematic of our apparatus is shown in Fig. 2. We removed approximately 10 cm of the jacket from the fiber and attached one end to the rotating motor and the other end to a stationary V-groove. This fixed end was held such that the fiber would not rotate at this point. At the other end of the fiber a motor rotated at a constant speed. A tungsten ribbon, that nearly surrounds the hi-bi fiber as shown in Fig. 2, is used to heat the fiber. As shown in Fig. 2 argon gas both cooled and protected the tungsten ribbon from the surrounding air, and the hi-bi fiber was stabilized with a vacuum V-groove on either side of the heater. We heated the fiber to near-melting temperatures (~1400–1600 °C) while the rotating motor twisted the fiber. This high temperature annealed out any stress induced in the fiber, due to the elasto-optic effect, associated with the initial twisting. Water cooling kept the fixture housing from overheating.

At the same time the fiber was being twisted and heated, a second motor advanced the heating element along the length of the fiber, shown in Fig. 2. The second motor speed is varied to obtain a certain twist-rate profile along the length of the hi-bi fiber. Both motors and the filament current were controlled by a

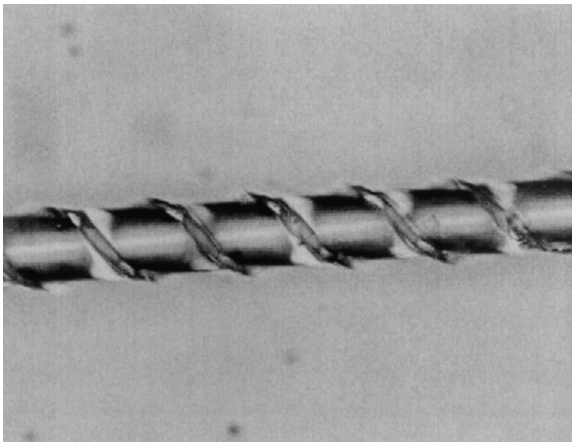

Fig. 3. Photograph of a twisted and heated fiber showing the corkscrew shape and microbending.

computer to obtain low-loss PT fibers with the desired twist-rate profile. An apparatus with constant motion and varying rotation rate could be used as well.

For best results we began with a constant level of twist per millimeter (one twist equals 2π rad of rotation) for a length of approximately 2 mm and then began the desired twist-rate profile. After heating and twisting, we placed the fiber in a capillary and polished back 2 mm or more into the PT fiber because this beginning region usually had high loss, possibly because of fiber microbending when the process was initiated. The apparatus shown in Fig. 2 held the hi-bi fiber in a straight line with the vacuum V-grooves and the tension between the fiber holder and the rotating motor. This apparatus kept the fiber, to a certain extent, from taking on a corkscrew shape when twisted and heated. Microbend losses become significant in fibers with a corkscrew shape. Figures 3 and 4 show photographs of fibers twisted without any support and with the vacuum V-groove apparatus, respectively. The corkscrew shape of the fiber in Fig. 3 does not guide light. Figure 4 shows a

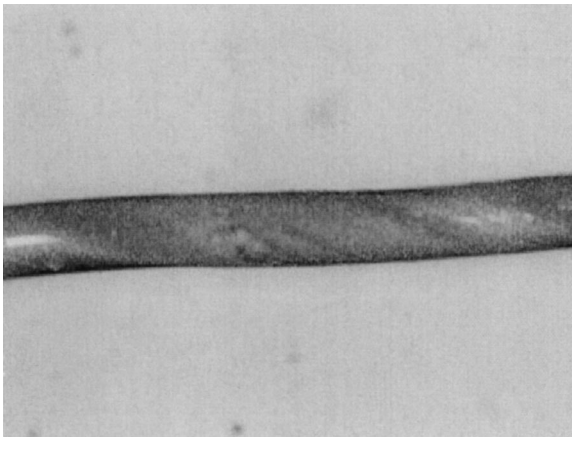

Fig. 4. Photograph of a PT fiber sample with a minimum of microbending or corkscrew shape. The fiber has a dark surface because of a glass–air–tungsten reaction. Also, crystal growth is evident by the grainy surface of the fiber.

better fiber, but the heating process initiated devitrification, as indicated by the grainy surface.[4] The surface of the fiber was also discolored from reactions with the air and tungsten. This fiber could be reheated to remove some of the devitrification and increase its overall strength.

3. Theoretical Evaluation of Polarization-Transforming Fiber

We used the Runge–Kutta method to numerically solve the coupled-mode equations for variable coupling to guide the manufacture of fibers using different twist-rate functions $\tau(z)$, total lengths L_R, and beginning twist rates $\tau(0)$.[2,3] The coupled-mode equation for variable coupling is

$$\frac{\mathrm{d}A(z)}{\mathrm{d}z} = K(z)A(z), \qquad K(z) = \begin{bmatrix} j\,\dfrac{\Delta\beta}{2} & \tau(z) \\ -\tau(z) & -j\,\dfrac{\Delta\beta}{2} \end{bmatrix}, \tag{1}$$

where A is a vector whose elements A_x and A_y are, respectively, the horizontally and vertically polarized local modes in the fiber and $\Delta\beta$ is the phase velocity difference between the two modes.[2,3,5] To solve Eqs. (1) we can use the same transformation method as used in previous constant-twist cases, with the expression $A(z) = O(z)W(z)$, where $O(z)$ is the diagonalizing matrix and $W(z)$ is the eigenmode vector. However, $O(z)$ now has variable elements:

$$O(z) = \begin{bmatrix} \cos\phi(z) & i\,\sin\phi(z) \\ i\,\sin\phi(z) & \cos\phi(z) \end{bmatrix}, \tag{2}$$

where $\phi(z) = 0.5\,\tan^{-1}[2Q(z)]$, $Q(z) = \tau(z)/\Delta\beta = L_b/L_S(z)$, L_b is the phase beat length, and $L_S(z)$ is the variable spin pitch of the fiber. The elements of $W(z)$ no longer separately satisfy independent differential equations and do not have an exact closed-form expression, but are coupled functionally by the term $\mathrm{d}\tau(z)/\mathrm{d}z$. (These equations have been previously solved by Huang.[2,3]) We solved Eqs. (1) numerically with the Runge–Kutta method and with Volterra's multiplicative integral method[6,7] and found no significant difference in the results. We solved them for the situation in which circularly polarized light is launched into the fast-spun end of the PT fiber. For this situation the input of left-circularly polarized light will be transformed into vertical-linearly polarized light by the PT fiber. A measure of the effectiveness of the transformation is the extinction ratio of the output linear polarization state, which is also easier to experimentally verify. We assumed a perfect circular polarization state for the normalized input, and the extinction ratio was determined by the function

$$E_R(z) = -10\,\log_{10}\left[\frac{|A_x(z)|^2}{|A_y(z)|^2}\right], \tag{3}$$

where $A_x(z)$ and $A_y(z)$ are the linearly polarized local modes along the length of the fiber. For a perfect PT fiber the circular-to-linear transform would yield an $E_R(z) = \infty$ at $z = 0$. (We define $z = 0$ as the fast-spun end of the fiber and $z = L_R$ as the end of the fiber with no twist.)

A variety of twist-rate profiles were used to make the PT fibers: linear, exponential, and cosine. These are not inclusive, but are representative only of the twist-rate functions that could be used. However, each function poses a different set of experimental constraints that must be considered to achieve a practical PT fiber with an extinction ratio greater than 20 dB and a length shorter than 50 mm. $\tau(0)$, the beginning twist rate, can be in units of radians per millimeter or twists per millimeter where one twist equals 2π rad. The functions below are in radians per millimeter and are converted to twists per millimeter for Figs. 5 and 6.

The linear twist-rate function we used was

$$\tau_{Li}(z) = \frac{2\pi\tau(0)}{L_R}(L_R - z), \tag{4}$$

where $(L_R - z)$ is the length of the fiber from the zero twist end. Fibers made with this twist-rate function worked, but the best performance required long lengths and high twist rates that were not as desirable.

The exponential twist-rate function we used was

$$\tau_{\exp}(z) = 2\pi\tau(0)\exp\left(\frac{-az}{L_R}\right), \tag{5}$$

where a is an arbitrary constant. Unfortunately, variations in our apparatus prevented us from making a low-loss fiber using the exponential twist-rate function. The shape of the twist profile at the fast-spun end would have to be well controlled because of the rapid change in $\tau_{\exp}(z)$. This exponential profile was impractical given the number of experimental parameters involved in the process of heating, twisting the hi-bi fiber, and the difficulty in controlling these parameters with our apparatus. Possibly with a refined apparatus this twist profile could be used successfully.

The cosine twist-rate function we used was

$$\tau_{\cos}(z) = \pi\tau(0)\left[1 + \cos\left(\frac{\pi z}{L_R}\right)\right]. \tag{6}$$

The PT fiber with a cosine twist rate is interesting because the derivative of $\tau_{\cos}(z)$ is 0 at both ends of the fiber. This may reduce the effects of variations in the experimental parameters at the high-twist end of the PT fiber. We had the most success experimentally with this cosine twist profile of PT fiber.

4. Predicting the Theoretical Temperature and Wavelength Dependencies of the Polarization-Transforming Fiber

As mentioned above, PT fibers rely on the internal stress birefringence in the hi-bi fiber to convert polarization states from linear to circular local modes. If that birefringence changes, due to a temperature or wavelength change, then the properties of the PT fiber will change as well. To predict the temperature and wavelength dependencies of a PT fiber, we modeled the extinction ratio $E_R(z)$ versus a change in the beat length L_b of the hi-bi fiber where the length L_R, the maximum twist rate $\tau(0)$, and the twist-rate function were fixed. The beat-length variation was then attributed to a change either in temperature or in wavelength. The beat length of a hi-bi fiber is $L_b = 2\pi/\Delta\beta$ where $\Delta\beta = 2\pi\Delta n/\lambda$ is the linear phase shift per unit length and Δn is the linear birefringence. As shown in Eq. (7), the beat length of a hi-bi fiber depends on wavelength and temperature:

$$L_b(\lambda, T) = \frac{\lambda}{\Delta n(\lambda, T)}, \tag{7}$$

where T is the temperature, λ is the wavelength, and $\Delta n(\lambda, T)$ is the linear birefringence in the fiber as a function of wavelength and temperature. Thus the normalized wavelength and temperature dependencies of the beat length can be expressed by Eqs. (8):

$$\frac{1}{L_b}\frac{dL_b}{d\lambda} = \frac{1}{\lambda} - \frac{1}{\Delta n}\frac{d\Delta n}{d\lambda},$$
$$\frac{1}{L_b}\frac{dL_b}{dT} = -\frac{1}{\Delta n}\frac{d\Delta n}{dT}. \tag{8}$$

The values of $(1/\Delta n)d\Delta n/d\lambda$ and $(1/\Delta n)d\Delta n/dT$ have been measured and reported by several authors and found to be approximately -8.3×10^{-5} nm^{-1} and 1.2×10^{-3} °C^{-1}, respectively.[8,9] From Eqs. (8) a change in beat length can be attributed to changes in temperature or wavelength.

Before we compare the estimated and experimental temperature and wavelength dependencies, another conversion from extinction ratio to retardance error is useful. (The retardance of a section of PM fiber is defined as $\delta = \Delta\beta l = 2\pi\Delta n l/\lambda$, where l is the section length.) A PT fiber can be simplistically modeled as a quarter-wave retarder for comparison with a PM fiber retarder. For a perfect quarter-wave retarder, with retardance $\delta = \pi/2$, the conversion from a circular to a linear polarization state would lead to an infinite extinction ratio for the output linear polarization state. If the retarder has a retardance that is slightly different from $\pi/2$ with a retardance error ε', then the extinction ratio of the linear polarization state will be less than infinity. The retardance error $\varepsilon' = \delta - \pi/2$ can be determined from the linear polarization-state extinction ratio E_R as shown in Appendix A, relation (A4).

From Eqs. (1)–(8) and Huang's theory[2,3] we estimated the temperature and wavelength dependen-

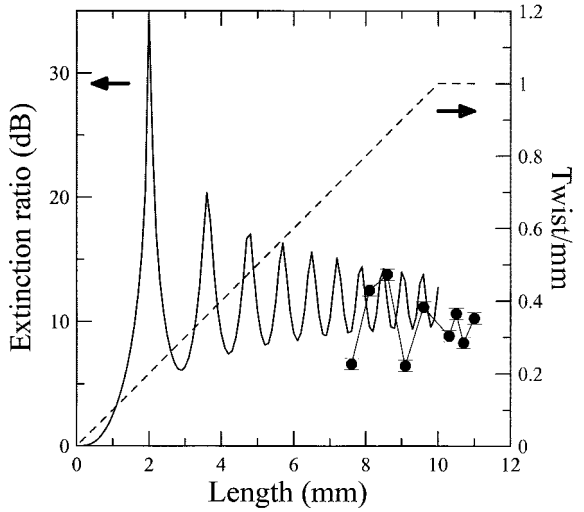

Fig. 5. Theoretical (solid curve) and measured (filled circles) extinction ratio for a PT fiber made with a linear twist-rate profile with $\tau(0) = 1$ twist/mm $L_R = 10$ mm, and length is $(L_R - z)$. The twist rate for this fiber is shown as a dashed curve.

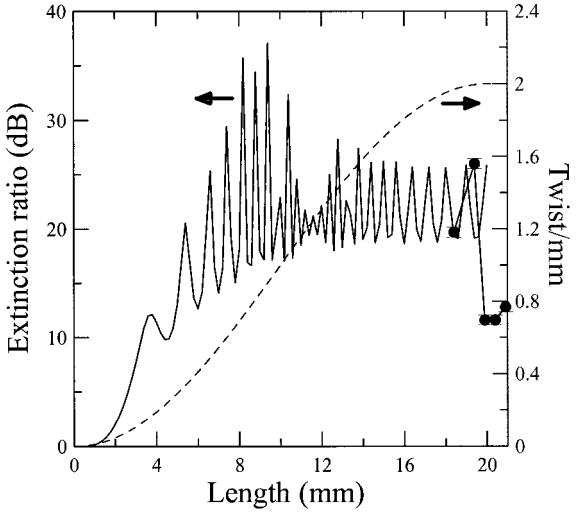

Fig. 6. Theoretical (solid curve) and measured (filled circles) extinction ratio for a PT fiber made with a cosine twist-rate profile with $\tau(0) = 2$ twists/mm, $L_R = 20$ mm, and length is $(L_R - z)$. The twist rate for this fiber is shown as a dashed curve.

cies for PT fibers made with the linear, exponential, and cosine twist profiles. Figures 5–8 show the measured and calculated effect of cutting back into the PT fiber and changes in temperature or wavelength on the extinction ratio or retardance error ε'.

5. Experimental Results

To determine the PT properties of our PT fibers we launched a nominally (97%) circular polarization state into the fast-spun end of the fiber and, with a polarizer, measured the extinction ratio of the linear output polarization state. We used lasers at 1.3 and 1.55 μm to measure the wavelength dependence, but we measured the fibers primarily at 1.3 μm. The single-mode bow-tie hi-bi fiber we used was 125 μm in diameter, had a beat length $L_b \approx 4$ mm at 1.3 μm, a 0.11 numerical aperture, and a 9-μm mode field diameter.

Using the apparatus discussed above, we manufactured several PT fibers with various twist-rate profiles and lengths. As mentioned above the most successful twist-rate profile was the cosine, described in Eq. (6). Using this profile, we made fibers with extinction ratios (for the circular-to-linear conversion) greater than 20 dB and with losses below 1 dB. We also tried making PT fibers with linear and exponential profiles, but either the extinction ratio was less than 20 dB or the loss of the fiber was greater than 5 dB, or both.

To evaluate the performance of the PT fiber, we polished back from the start of the twist until both the loss and the extinction ratio were acceptable. This polish-back method could also be used to confirm the twist-rate model for the fiber. Figure 5 shows a PT fiber with a linear twist-rate profile, with $\tau(0) = 1$ twist/mm and $L_R = 10$ mm. As the PT fiber is polished back, the extinction ratio of the linear output state fluctuates with an amplitude near that of the amplitude fluctuation of the theoretical extinction ratio prediction. Because of uncertainties in the polish-back length and the start-of-twist location on the fiber, agreement can be only approximate. The PT fiber in Fig. 5 is not a good candidate because of the loss, approximately 5 dB, and because the extinction ratio is less than 10 dB.

Another PT fiber was made with the cosine twist rate and is shown in Fig. 6. This fiber had $\tau(0) = 2$ twists/mm and $L_R = 20$ mm, with a loss of approximately 6 dB and approximately a 20-dB extinction ratio. Again, once the fiber was polished back into the cosine twist-rate profile, the measured extinction ratio of the PT fiber matched the theoretical predictions for absolute value and oscillation. The first few data points are in the region where the twisting had just begun, are not easily modeled, and have high loss.

We manufactured several fibers using the cosine twist rate, with $\tau(0) = 1.5$ twists/mm and $L_R = 30$ mm. For our apparatus, this type of PT fiber had the lowest loss, less than 1 dB, for an extinction ratio greater than 20 dB. With these fibers we tested the temperature and wavelength dependencies of the extinction ratio of a PT fiber. Figure 7 shows our results of measuring the extinction ratio of the linear output polarization state at approximately 1318 and 1555 nm when a circular state was input on the fast-spun end of the PT fiber sample. Repeated measurements were made, and the error bars in Fig. 7 represent twice the standard deviation of that set of measurements. The theoretical values have a −3.3-dB bias for comparison purposes. Our samples of PT fiber can have an extinction ratio lower than predicted, possibly because of imperfections in our process, but should still follow the predicted wave-

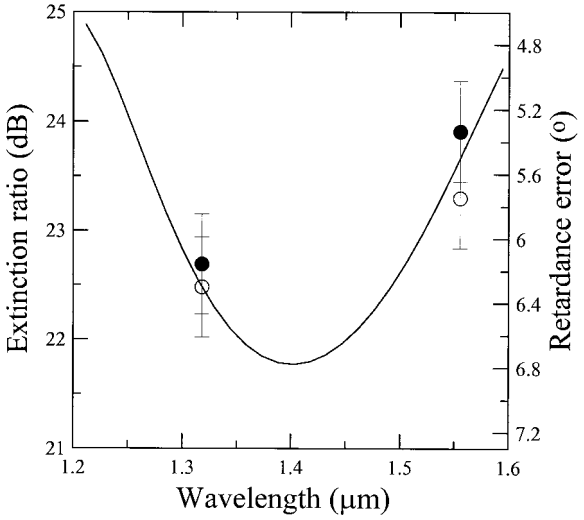

Fig. 7. Theoretical (solid curve) and measured (filled and open circles) extinction ratio for a PT fiber made with a cosine twist-rate profile with $\tau(0) = 1.5$ twists/mm and $L_R = 30$ mm. Theory was biased by -3.3 dB to match the 1.55-μm data. Two PT fiber samples (solid and filled circles) made under the same conditions were used. The estimated retardance error is shown in the right vertical axis.

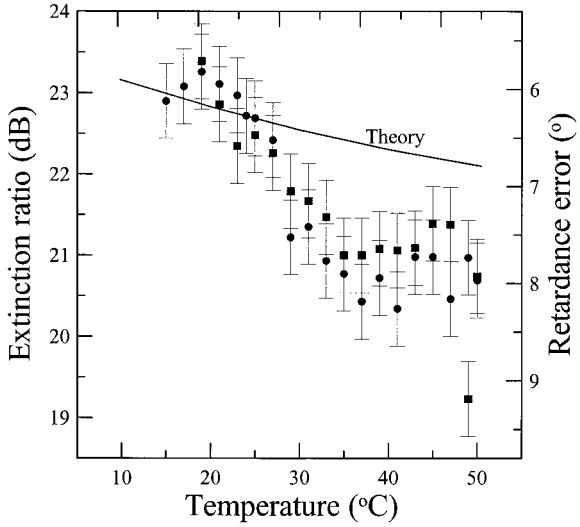

Fig. 8. Theoretical (solid curve) and measured (filled circles) extinction ratio of two PT fibers (filled circles and filled squares) and versus temperature at 1.3 μm. A bias of -3.3 dB was added to the theoretical values. Also, the estimated retardance error is shown on the right vertical axis.

length dependence. In Fig. 7 the experimental values do match the biased theory well. Also, shown in Fig. 7 is an estimate of the retardance error from a perfect quarter-wave plate. The retardance error was determined from the biased theory by use of Eq. (A4).

To measure the temperature dependence of the extinction ratio of the fiber, we heated and cooled samples on a thermo-electric cooler while measuring the extinction ratio of the linear output polarization state. A circular input polarization state was launched into the fast-spun end of the PT fiber, and the extinction ratio of the linear output polarization state was recorded. Figure 8 shows the temperature dependence of the extinction ratio of two PT fiber samples compared with the theoretical prediction. Again, the theoretical values were biased by -3.3 dB. The PT fiber samples have a larger extinction ratio temperature dependence than the theory predicts, which may be due to stress induced by the capillary housing. Figure 8 also has an estimate of the retardance error from a perfect quarter-wave plate. The measured normalized temperature dependence of these samples is $6 \times 10^{-4}\ °C^{-1}$, larger than the theoretical slope of $2 \times 10^{-4}\ °C^{-1}$.

6. Conclusions

We have taken Huang's theoretical treatment of the PT fiber and made short lengths of fiber (<30 mm) with low loss to show that the PT properties of the fiber can be maintained. However, the performance of the shorter-length fiber now depends strongly on the shape of the twist-rate function. We also developed a postdraw method for manufacturing these fibers and have shown that a 30-mm sample can have a circular-to-linear polarization-mode conversion greater than 20 dB with a loss of less than 1 dB.

We have compared the PT fiber with a conventional hi-bi fiber quarter-wave plate for the case in which the polarization-mode conversion capability of the PT fiber is similar to that of a quarter-wave plate when linearly polarized light is changed to circular polarized light, and visa versa. Table 1 shows the nor-

Table 1. Normalized Dependencies of Retardance for Temperature and Wavelength Changes for PT and Conventional Quarter-Wave Plate Fibers

Fiber Type	Normalized Temperature Dependence $[(1/\delta)d\delta/dT]$ $(°C^{-1})$ at 1.3 μm	Normalized Wavelength Dependence $[(1/\delta)d\delta/d\lambda]$ (nm^{-1}) at 1.3 μm
Bow tie	1.2×10^{-3}[a]	7×10^{-4}[b]
Elliptical core	0.9×10^{-3}[c]	7×10^{-4}[b]
Elliptical core	0.2×10^{-3}[d]	7×10^{-4}[b]
PT (experimental)	0.6×10^{-3}	1.4×10^{-4}
PT (best theoretical)	-2×10^{-5}	-3×10^{-5}

[a]Reference 8.
[b]Estimated value.
[c]Reference 9.
[d]Reference 10.

malized dependencies of retardance δ (from either Δn or the measured extinction ratio) for temperature and wavelength changes for conventional fiber quarter-wave plates and the PT fiber. (As stated above, the temperature or wavelength dependence of a quarter-wave plate is attributable to the direct change in Δn, whereas the temperature or wavelength dependence of the extinction ratio of a PT fiber operating in a circular-to-linear polarization-state conversion is indirectly dependent on Δn.) The wavelength dependence for the conventional quarter-wave plates was determined from Eqs. (8). The temperature dependence has been measured by various authors, and depending on the fiber type, the temperature dependence varies from $1.2 \times 10^{-3}\ ^{\circ}\mathrm{C}^{-1}$ to $0.2 \times 10^{-3}\ ^{\circ}\mathrm{C}^{-1}$.[8–11]

The experimental PT fiber discussed in Table 1 is also shown in Figs. 7 and 8. The fiber has a cosine twist-rate function with $\tau(0) = 1.5$ twists/mm and $L_R = 30$ mm. The theoretical PT fiber discussed in Table 1 has a length of 300 mm with a cosine twist-rate function and $\tau(0) = 1.5$ twists/mm. The longer PT fiber has lower predicted wavelength and temperature dependencies for the extinction ratio. This illustrates that the temperature and wavelength dependencies of a PT fiber can be tailored by length and twist-rate profile. As shown in Fig. 8 the wavelength dependence changes sign between 1.3 and 1.55 μm. The temperature dependence will also have a different sign at the two different wavelengths.

The PT fiber we made and show in Figs. 7 and 8 has a substantially better wavelength performance as compared with the conventional fiber quarter-wave plate by use of the same fiber type. When compared with the conventional fiber quarter-wave plate, the variation with wavelength is a factor of 5 better for the PT fiber we made, or a theoretical factor of 23 for a 300-mm length PT fiber. The temperature dependence of the 30-mm sample has a value comparable to that of conventional quarter-wave plates, and the 300-mm length PT fiber has a predicted value ten times better than the best reported value for a conventional quarter-wave plate.

Because of the tunable wavelength and temperature performance of a PT fiber, there are some interesting applications. One is a stable fiber quarter-wave plate for polarimetric metrology. However, the present samples do not compare with the standard retarder produced by the National Institute of Standards and Technology.[12] Another possible application is optical fiber current sensors.[10,11,13] The fiber Sagnac and in-line Sagnac current sensors require a fiber quarter-wave plate to convert linear polarization modes in the interferometer into circular polarization modes to sense current flowing through the aperture of the sensing fiber coil. The temperature dependence of the fiber quarter-wave plate can be used to compensate for other temperature-dependent components and physical effects in the sensor, thus stabilizing the sensor for commercial use.[10,11,13] With a PT fiber the required compensation could be tuned for optimal sensor stability over temperature and possibly source wavelength changes.

In summary the PT fiber can have a performance comparable to that of a conventional hi-bi fiber quarter-wave plate. However, the PT fiber can be tailored, by length and twist-rate profile, to have better wavelength and temperature performance than the conventional fiber quarter-wave plate. Also, the PT fiber can be made to have the opposite sign for its temperature and wavelength dependencies compared with a conventional fiber quarter-wave plate as shown in Figs. 7 and 8.

Appendix A: Retardance Error

A PT fiber, in the arrangement where a circular polarization state is converted to a linear polarization state, can be modeled as a quarter-wave retarder where the retardance is $\delta = \pi/2 + \varepsilon'$, with ε' as the retardance error. If we launch a polarization state of some ellipticity into the quarter-wave plate, a linear polarization state with some extinction ratio E_R will exit the device. This arrangement can be modeled with Jones's calculus in the following manner.[14] The output Jones's vector for an elliptically polarized state, angle 0°, launched into a wave plate and then analyzed by a polarizer can be found by the following:

$$\begin{bmatrix} A_x \\ A_y \end{bmatrix} \cong \frac{1}{2}\begin{bmatrix} 1 & \pm 1 \\ \pm 1 & 1 \end{bmatrix} \times \begin{bmatrix} \exp(i\delta/2) & 0 \\ 0 & \exp(-i\delta/2) \end{bmatrix} \frac{\sqrt{2}}{2}\begin{bmatrix} -i \\ 1 - \varepsilon_C \end{bmatrix}, \tag{A1}$$

where the wave-plate's axis is at 0°, the polarizer's axis is at ±45°, and ε_C is a small deviation from circular polarization ($|A_x|^2 \cong |A_y|^2 - 2\varepsilon_C$). The measured intensities from the two orientations of the polarizer are

$$I_{\pm} \cong \frac{1}{4}[1 + (1 - \varepsilon_C)^2 \pm 2(1 - \varepsilon_C)\cos\varepsilon']. \tag{A2}$$

The extinction ratio of the measured intensities is

$$E_R = \frac{I_-}{I_+} \cong (1 - \varepsilon_C)\frac{\varepsilon'^2}{2}, \tag{A3}$$

for small ε_C and ε'. Thus, for a given input polarization state (that is nearly circular) and an extinction ratio, a retardance error can be determined. The retardance error is

$$\varepsilon' \cong \left[\frac{2E_R}{(1 - \varepsilon_C)}\right]^{1/2}. \tag{A4}$$

Relation (A4) can be used to determine the retardance error for a PT fiber from the input circular polarization-state error and the extinction ratio of the output linear polarization state.

The effect of the input circular polarization-state error can be seen in relation (A4) as a bias to ε'. Our

input polarization state had ε_C equal to approximately 3%. This would bias E_R by approximately 0.1° for E_R values below 20 dB. The bias due to ε' is negligible for higher E_R values.

References

1. A. J. Barlow, J. J. Ramskov-Hansen, and D. N. Payne, "Birefringence and polarization mode-dispersion in spun single-mode fibers," Appl. Opt. **20,** 2962–2968 (1981).
2. H.-C. Huang, *Microwave Approach to Highly Irregular Fiber Optics* (Wiley, New York, 1998), Chap. 7 and Appendixes A, B, and C, pp. 198–295.
3. H.-C. Huang, "Fiber-optic analogs of bulk-optic wave plates," Appl. Opt. **36,** 4241–4258 (1997).
4. A. H. Rose, "Devitrification effects in annealed optical fiber," J. Lightwave Technol. **15,** 808–814 (1997).
5. R. C. Jones, "A new calculus for the treatment of optical systems. VII. Properties of the *N*-matrices," J. Opt. Soc. Am. **38,** 671–685 (1948).
6. G. Birkhof and G.-C. Rota, *Ordinary Differential Equations*, 4th ed. (Wiley, New York, 1989).
7. M. C. Pease, *Methods of Matrix Algebra* (Academic, New York, 1965).
8. K. Okamoto, T. Kdahiro, and N. Shibata, "Polarization properties of single-polarization fibers," Opt. Lett. **7,** 569–571 (1982).
9. A. Ourmazd, M. P. Varnham, R. D. Birch, and D. N. Payne, "Thermal properties of highly birefringent optical fibers and preforms," Appl. Opt. **22,** 2374–2379 (1983).
10. S. X. Short, A. A. Tselikov, J. U. de Arruda, and J. N. Blake, "Imperfect quarter-wave plate compensation in Sagnac interferometer-type current sensors," J. Lightwave Technol. **16,** 1212–1219 (1998).
11. K. Bohnert, P. Gabus, and H. Brandle, "Temperature and vibration insensitive fiber-optic current sensor," in *14th International Conference on Optical Fiber Sensors*, A. G. Mignani, ed., Proc. SPIE **4185,** 336–339 (2000).
12. K. B. Rochford, A. H. Rose, P. A. Williams, C. M. Wang, I. G. Clarke, P. D. Hale, and G. W. Day, "Design and performance of a stable linear retarder," Appl. Opt. **36,** 6458–6465 (1997).
13. K. Bohnert, P. Gabus, J. Nehrigh, and H. Brandle, "Temperature and vibration insensitive fiber-optic current sensor," J. Lightwave Technol. **20,** 267–276 (2002).
14. W. A. Shurcliff, *Polarized Light: Production and Use* (Harvard University, Cambridge, Mass., 1962).